

# The Electric Response of Wood for Guitar Pickups Using Surface Acoustic Wave Transducers

Samuel C. Jung<sup>1</sup>

Dr. Ryan S. Westafer<sup>2</sup>

Professor William D. Hunt<sup>3</sup>

---

<sup>1</sup> Woodward Academy, Atlanta, GA

<sup>2</sup> Advanced Concepts Laboratory (ACL), Georgia Tech Research Institute (GTRI)

<sup>3</sup> School of Electrical and Computer Engineering, Georgia Institute of Technology

**Abstract:**

During live concerts, the sound from acoustic guitars becomes distorted when amplified at a high level. Wood exhibits a weak piezoelectric effect; we fabricated and tested a piezoelectric pickup electrode design that leverages this response to amplify the guitar based on the vibrations of the wood itself, rather than traditional pickups which amplify the guitar's strings. When the mechanical vibrations on the guitar's soundboard are collected through an interdigitated transducer (IDT), amplified, and converted to sound, one can express the "true" sound of the guitar.

We examined previous works, created a model, and tested various electric responses for an acoustic guitar's soundboard with a simple transducer to verify this surface behaves similarly to wood. Next, we designed and validated the functionality of an IDT against materials with known dielectric constants. This IDT was then modeled and tested for the same electric responses as our simple transducer. To predict the soundboard's displacements and determine the ideal placement for the IDT to pickup maximum voltage from the soundboard, we developed a third model. A scalable and aesthetic method for printing conductive electrodes was proposed, and the longevity of such pickups was also established.

Our experiments yielded a quantifiable voltage response from z-directed distortions on the guitar's soundboard. This work presents a comprehensive design methodology for the pickup technology to be easily replicated and extended towards other classes of instruments (strings, brass, and percussion); it also aims to propose a responsive interface that functions as both a visually captivating and low-cost method for musicians to amplify instruments for their audience.

## 1. Introduction

When the strings for acoustic guitars are amplified, at a certain volume threshold-- for instance, during live concerts-- it is often difficult to differentiate between a high-quality instrument and a mass-produced instrument made for intermediate musicians. The objective of this work is to examine the electric properties of wood to propose a new method of amplifying the guitar, which can be extended to other wood based instruments.

Pickups serve an important role in the effective amplification of musical instruments, most notably the guitar. Most guitar pickups function like microphones which are placed in close proximity to the strings. Depending on the position, sensitivity width, string dispersion, string impedance, and the mixing effect of multiple pickups, unique timbre characteristics of varying quality can be achieved for acoustic guitars [1]. On the other hand, guitar pickups can also function via transducers which convert the string vibrations of the instrument to electric signals. Acoustic guitars will often use a string piezoelectric pickup to achieve this result specifically. Our proposed pickup aims to amplify and convert the vibrations of the wood, rather than the vibrations of the strings, to express the “true” sound of the instrument.

The piezoelectric effect is the occurrence of electric polarization which is achieved through the application of mechanical stress on a plane. The magnitude and direction of the electric charges can also be manipulated depending on the location, direction, and intensity that stress is applied [2]. Piezoelectricity is traditionally associated with crystalline materials; however, it has also been shown that materials with crystal-like, cellulose, and polymer structures-- wool, human hair, bone, and wood-- also exhibit a piezoelectric effect. Wood in particular displays weak but measurable piezoelectric characteristics, with its constants  $-d_{14} = d_{25}$  being approximately 5% of the  $d_{11}$  piezoelectric constant of quartz [3]. The electric properties exhibited by wood can further be modified by manipulating shear forces and moisture content, while also taking into account the grain direction, wood species, and external chemical treatments.

$$\begin{bmatrix} P_1 \\ P_2 \\ P_3 \end{bmatrix} = \begin{bmatrix} 0 & 0 & 0 & d_{14} & 0 & 0 \\ 0 & 0 & 0 & 0 & d_{25} & 0 \\ 0 & 0 & 0 & 0 & 0 & 0 \end{bmatrix}$$

**Fig. 1.** The piezoelectric tensor for wood.

Within the tensor in figure 1,  $P$  stands for a component of the piezoelectric polarization vector, while  $d$  is the strain coefficient. The strain coefficient is expressed with two subscripts, with the first subscript indicating the direction of the electric field while the second subscript represents the direction of mechanical stress or strain.

Surface acoustic waves (SAWs), also known as Rayleigh waves, are sound waves with a vertical shear and longitudinal component. When they travel along an elastic surface, SAW sensors can be used to determine traits like mass, temperature, and other mechanical properties. The applications for SAW devices vary widely from sensing drag friction in aerospace, detecting ice formation on aircraft wings, and determining the structural integrity of large construction projects like bridges [4]. The advantage of using SAW sensors opposed to other devices is that SAW devices are known to be extremely accurate, stable, and can usually be produced at a low cost.

This project uses SAW filters to convert electric energy into acoustic energy with the use of a piezoelectric substrate using a structure known as the interdigitated transducer (IDT). IDTs are unique in that they can control the frequency and extent to which electric signals are converted to acoustic energy by manipulating the fixed metallization pattern that they are made of. The typical design of an IDT consists of a fixed metallization pattern, with a terminal for an input or output signal. A SAW device will usually be structured with an input IDT, a delay line, and output IDT, which are all implemented on top of the piezoelectric substrate [5].

The wood grain direction also affects piezoelectric tensor values, but they have a negligible impact on these values in this experiment. When measured at the fundamental resonance, the displacements on the backplate of the guitar are also negligible; they are proportionally insignificant when compared to the top soundboard of the guitar [6]. Although the first resonance of guitars usually occurs between 90-120Hz, the second mode which lies between

170-250Hz is significant because this is the fundamental mode of the guitar's soundboard itself [7].

For the purposes of this research, I focused on attaching SAW pickups to the guitar's soundboard itself. Because IDTs are fabricated based on wavelength, and they do not possess a wide operating frequency range compared to the range of audible sound, I used a chain of IDTs to assemble a singular sound output. Thus, it is important to understand the vibrating frequency range of wood as well as guitar soundboards in order to determine the range that the IDTs should operate on. The frequency range of classical guitars varies from 65 Hz-2 kHz, which is just above the sub-bass frequency band of 20-60 Hz that is usable in audio recordings [8], with harmonic notes of the acoustic guitar reaching up to the 20 kHz frequency range which lies on the upper threshold of human hearing [9].

Holographic interferometry is a technique in which one shines lasers on an optically rough surface to determine displacements on the object being measured. These measurements can then be used to determine strain, stress, and other types of vibrational analysis as well. For this experiment, holographic interferometry was used to ascertain the exact locations of the minimum and maximum displacements. This information was then used to measure and design the electrodes for the guitar soundboard based on the excitations of the wood.

The greatest displacement on the guitar lies in its strings. However, it is also important to consider that the soundboard is mostly sympathetic with vibrations through the guitar's mount point, which is located on the bridge. Strain energy is the potential energy stored in a material when it is subjected to deformation. In this experiment, the most prevalent source of strain energy resulted from the bracing on the soundboard of the acoustic guitar along with the energy gained when the strings were played.

Standing waves were significant in this experiment because they were created at certain vibrating frequencies for strings. Harmonic frequencies for the guitar's strings could then be identified based on the location of these standing waves; the same principle can be extended towards the wooden soundboard's vibrations, too. Lamb waves are acoustic waves that are also important to identify because they function as elastic waves that propagate along the normal plane. Because lamb waves have no y-direction, they were ideal for modeling wood's vibrations in air, and the electric fields generated were mostly perpendicular towards the surface of the soundboard [10].

## 2. Materials, Methods, and Results

### 2.1 Overall Approach

	Criteria	Tool	Metric
Evaluation	Determining Pickup Position	Pyplot	Strain Energy Density & Voltage From Strain
	Designing Possible Electrodes	Inkscape (SVG) & Vibrometry	Voltage Response
Design	Wood, Rexolite, and Styrofoam Measurements	Microwave Frequency Analyzer	Impedance
	Electric Response of Wood Through Guitar Stimulation	Oscilloscope	Spectrum & Waveform Analysis
	Electrode Resistivity Over Time	LCR Meter	Capacitance & Resistance
	Long Term Viability of Printed Electrodes	Multimeter	Resistance

**Fig. 2.** The methodology of the research, technology used, and measurements conducted for each step.

### 2.2 Determining Pickup Position

To determine the pickup position, we required a model that would maximize voltage while considering other factors that would affect these measurements. In this experiment, we considered the wood species, moisture content for the soundboard, pre-stress, damping force, and acoustic phase velocity. Inta's work established that the acoustic guitar's soundboard vibrations can be modeled as a linear system at low amplitudes [11]. Although we found that the species of wood affects its piezoelectric coefficient, Fukada demonstrated that the differences in value ranged between  $0.1 \times 10^{-9}$  and  $3.5 \times 10^{-9}$ , negligible for our model [12]. Barkas found that decreasing wood's moisture content increased the electric resistance of wood; we were able to calculate the lamb wave velocity with the predicted shear and longitudinal wave velocities [13]. Pre-stress on wood had an interesting effect in that the voltage measured increased linearly within wood's elastic region while also exhibiting distinct peaks at the buckling and shearing

fracture points for wood [14]. We used  $d_{ik} = 3 \times 10^{-9}$  as the piezoelectric constant for our calculations, which was determined by Fukada [12] and supported by Bazhenov [3], and Zelinka's experiments [15].

Defining the x-y plane as the plane of the guitar's soundboard, we wanted to sum the electric field in this x-y plane for displacements in the z-direction due to the sound vibrations of the guitar to model the IDT's output. Specifically, we wanted to consider the electric field distribution of wood over space and the IDT's field distribution over space to model the soundboard's output voltage over air. While considering Nakai's experiment which showed strain is proportional to the displacements of the wood, and assuming space and frequency independence, we also investigated whether there was some unknown factor between electrode pairs which showed a measured potential energy that would result as a scalar value at that given frequency.

If  $E_x$  represents the x-directed electric field, it follows that:

$$E_x = d_{xz} \cdot u_z \quad (1)$$

Where  $d_{xz}$  represents the tensor coefficient mapping the z-directed displacement,  $u_z$ , to the x-directed field  $E_x$ .  $u_z$  can be modeled as the function:

$$u_z(x) = \sin(\beta x)$$

With  $\beta$  as the wavenumber,  $f$  as the frequency, and  $v_p$  as the acoustic phase velocity:

$$\begin{aligned} \beta &= \frac{\omega}{v_p} \\ \omega &= 2\pi f \\ \beta &= \frac{2\pi f}{v_p} \end{aligned} \quad (2)$$

We can then integrate the surface's z-directed displacement profile,  $u_z(x)$ , over the distance  $x$  for each frequency where  $x$  represents the propagation distance within the plane of the soundboard,  $z$  represents the normal propagations to the soundboard, and  $\zeta$  represents the damping force coefficient.

$$\begin{aligned}
& \int_{x_{t \min}}^{x_{t \max}} \zeta \cdot u_z(x, f) dx \\
&= \int_{x_{t \min}}^{x_{t \max}} \zeta \cdot \sin(\beta x) dx \\
&= -\frac{\zeta v_p}{2\pi f} \left( \cos\left(\frac{2\pi f x}{v_p}\right) \right) \Big|_{x_{t \min}}^{x_{t \max}}
\end{aligned} \tag{3}$$

Assuming the average width of a guitar soundboard is 0.5 meters, shown by the green line in figure 3 below. For the following data, the location  $x = 0$  on the soundboard was defined as the pink dot on figure 5. We integrated over the green line on figure 4 as well. The frequency used in all calculations was 214 Hz-- roughly half the frequency of "A" above middle C, a note that rests at 440 Hz.  $V_p$  was assumed to be 220 m/s. The integrated z-displacement of the soundboard is illustrated by figure 6. Figure 7 depicts the design of the electrode on which we based our calculations for this section. To calculate strain energy density for figure 8, we used Silker's calculation of  $700 \times 10^6$  pascals for the stiffness of the wood [16].

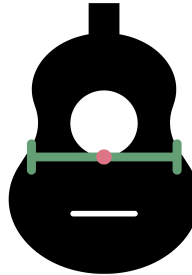


**Fig. 3.** The guitar's soundboard.

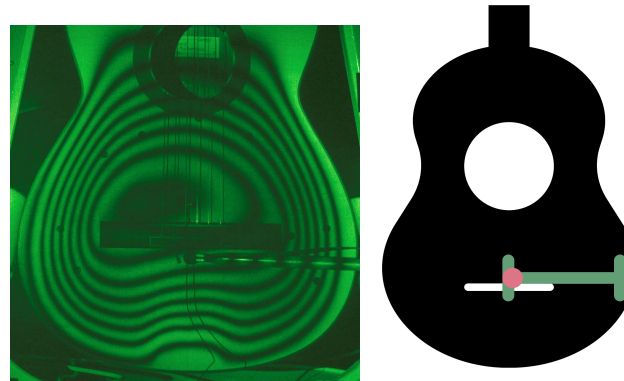


**Fig. 4. (left image)** Laser vibrometry on the soundboard [17] **Fig. 5. (right image)** Integrated area of guitar soundboard

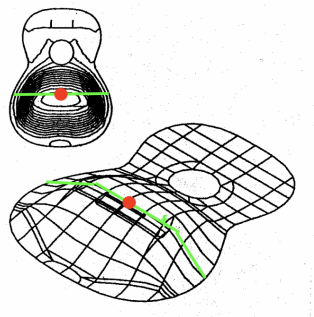


**Fig. 6.** Z-Displacement of guitar soundboard at the fundamental mode, annotated with a green line and dot to match fig. 3 and fig. 5 [18]

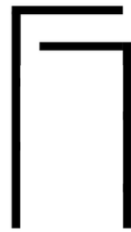


**Fig. 7.** Electrode for in-plane field pickup for the fundamental mode, shown in fig. 6.

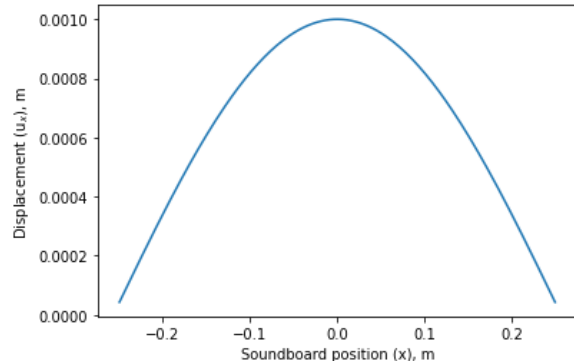


**Fig. 8.** Displacement (m) vs. Position on Soundboard (x), m

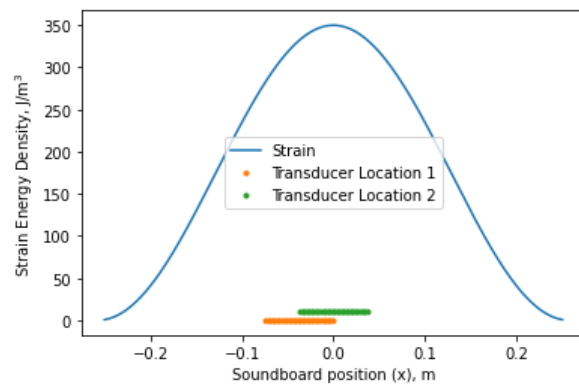


**Fig. 9.** Two Transducer Widths and Locations on the plot of Energy Density  $\text{J}/\text{m}^3$  vs. Position on Soundboard (x), m

As shown in figure 8, when our equation was integrated, the guitar's displacement was predicted to be greatest when the pickup was positioned at  $x = 0$  meters, with an overall z-displacement of 0.001 meters. Figure 9 shows that transducer locations #1 and #2 both concur that the maximum strain energy density, roughly  $350 \text{ J/m}^3$ , occurs when the pickup is positioned at  $x = 0$  meters on the soundboard.

### *2.3 Voltage Response, Capacitance, and Electrode Design*

The estimated voltage produced for a given stress on the soundboard can be modeled by the equation [3]:

$$d_{ik} = \frac{1635 \cdot 10^5 V C s_{\text{comp}}}{S_{\text{el}} P} \quad (4)$$

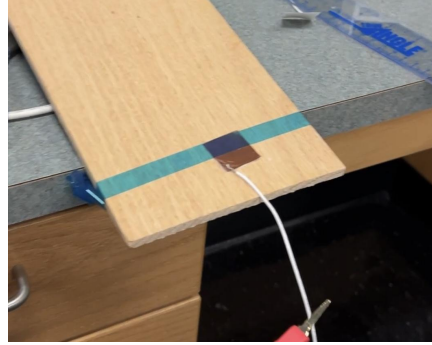
In equation 4,  $C$  represents the capacitance of the system while  $S_{\text{e}}$  represents the electrode surface area.  $S_{\text{comp}}$  refers to the surface area of compression,  $V$  represents the voltage, while  $P$  represents the pressure.  $1635 \times 10^5$  represents the conversion factor, and this specific formula uses the CGS system of units, with the notable exception of pressure being expressed in kilograms. Capacitance was derived from:

$$C = \frac{\epsilon_0 \epsilon_k s_{\text{el}}}{d} \quad (5)$$

Where  $\epsilon_0$  represents the dielectric permittivity and  $\epsilon_k$  represents the relative dielectric constant of wood.  $d$  stands for the thickness of the plate. Calculations for equation 5 were conducted in the MKS system of units.

First, it was necessary to create a simple model for a transducer to predict a capacitance, then verify the validity of this model. We used a parallel plate transducer to achieve this result.  $\epsilon_0$  was assumed as the constant  $8.854 \times 10^{-12}$ , and  $\epsilon_k$  was predicted to be 4.5, based on a measured relative room humidity of 46% by a Kestrel 5500 Weather Meter [19]. The surface electrode area

was  $6.35 \times 10^{-4}$  square meters, converted from an area of one square inch. We placed our transducer on a quarter inch thick piece of radially-cut wood, and converted this value to  $6.35 \times 10^{-2}$  meters for our calculations. From these values, our predicted capacitance was predicted to be 4.048 pF.



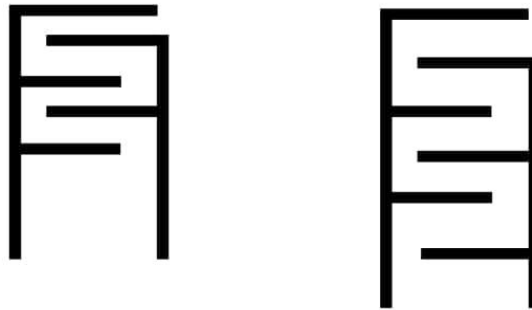
**Fig. 10.** Attaching the parallel plate transducer to confirm our capacitance model

Figure 10 illustrates how we attached our transducer on the wood. We used mylar tape, known for its low dielectric constant, to reduce any confounding variables on our measurements. The small-length white wire was also chosen specifically to minimize the least amount of capacitance introduced to our system. The actual capacitance was measured to be 3.9 pF, further validating our model with an error of 3.66%.

The guitar, shown below in figure 11, has a laminated spruce-topped soundboard [20]. James' work did not contain a dielectric constant for spruce; however, the piezoelectric modulus between oak and spruce wood differs by only  $2.9 \times 10^{-10}$ , based on Bazhenov's [3] experiments. Thus, we extrapolated James' dielectric constants for oak wood to our spruce-topped guitar. The guitar's soundboard was radially cut, and James' dielectric constant for radially-cut oak was 3.0 at room temperature and low humidity [19].  $S_{el}$  and  $\epsilon_0$  remained constant, and the thickness of the soundboard was measured to be 0.136 inches using a Mitutoyo 293-340-30 dial caliper. Converting this thickness to  $3.454 \times 10^{-3}$  meters, the predicted capacitance was 4.96 pF. The actual capacitance was measured at 4.73 pF, for an error of 4.6%. Our tests with the parallel plate capacitor confirmed that the wood of the guitar exhibits expected electric properties; a fact that was necessary to verify before modeling the voltage for a complex IDT. We wanted to ensure that the lamination on the guitar's soundboard would not affect our future measurements and analysis.



**Fig. 11.** Measuring the capacitance of our parallel plate transducer on a Yamaha F335



**Fig. 12.** The small and large IDT, exported as an SVG file

Figure 12 depicts the two IDT designs that were tested, with the small IDT on the left and large IDT on the right. Both designs were etched and cut on copper, which was then attached to Mitsubishi NB-RC-3GR120 resin-coated paper substrate. The capacitance recorded exists in figure 13 below.

	Small	Large
$C_R$ (pF)	58.7	35.0
$C_A$ (pF)	58.3	34.3

**Fig. 13.** The measured capacitance of our small and large transducer on air and Rexolite.

Rexolite was used because of its known dielectric constant, 2.53, compared to air which has a dielectric constant of 1. For these measurements, the cable capacitance was determined to be larger than 50 pF, and within the magnitude of 30pF. We connected our electrode through a

coaxial cable, and found that the effective surface area of the cable and small separation of conductors introduced an extra capacitance that dominated the actual capacitance of the electrodes themselves. Figure 14 depicts our setup. The data was inconclusive, so we modified our future experiments to use a cable that introduced a significantly lower capacitance, which we estimate to lie between 1-10 femto farads.

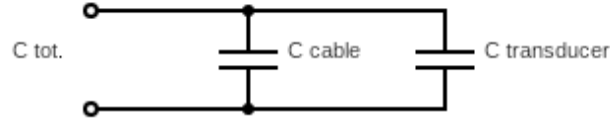


**Fig. 14.** Equivalent circuit model for cable connected to transducer

Next, a model was needed for the capacitance of our IDT. We surveyed several previous works including Mazlan and Ramli's model [21], Janeliauskas' work [22], and Hashimoto's textbook on SAW devices [23] to determine the best equation to estimate capacitance. Mazlan and Ramli's work did not adequately represent our IDT; they used a variation of the formula for calculating the capacitance of a parallel plate, which did not apply to our experiment. We eliminated Janeliauskas' model because his work detailed an elliptic integral that was ambiguously defined when calculated. Hashimoto's textbook contained the most comprehensive expression to calculate the capacitance for our IDT, which was:

$$\eta = \frac{w}{p_I}$$

$$C_s = W\epsilon(\infty) \frac{P_{-1/2}\{\cos(2\pi\eta)\}}{P_{-1/2}\{-\cos(2\pi\eta)\}} \quad (6)$$

We calculated capacitance for the large IDT.  $w$ , the width of a single IDT finger, was measured to be 0.005m.  $p_I$ , the electrode period was 0.025m. These two values were used to calculate  $\eta$ , the metallization ratio, or the fraction of metal width vs. gap width. We made the approximation:

$$\epsilon_\infty = \epsilon_0 \cdot \epsilon_{\text{Reff}} \quad (7)$$

Where  $\epsilon_0$  was the constant of the dielectric permittivity of free space, in  $\text{F}^*\text{m}^{-1}$ . We assumed  $\epsilon_{\text{Reff}}$  to be epsilon effective, holding a value between air and wood on the soundboard.  $W$  stood for the width of the IDT aperture, in other words, the length of the finger. The length  $W$  was 0.08m.

We evaluated the Legendre function,  $P_{1/2}$ , in Pyplot with our values to determine our capacitance using equation 6. However, Hashimoto's equation only calculates  $C_s$  as the static capacitance per a single IDT period. Our IDT had two periods, so our capacitance was double the value of  $C_s$ , producing a predicted value of 4.29 pF for our large transducer.

The actual capacitance of the large IDT on our guitar was 4.3 pF, for a 0.23% error from our predicted value. Using this capacitance, we rearranged equation 4 to predict voltage. The surface electrode area of the large transducer was measured to be 15.1 cm<sup>2</sup>. Assuming that the electrode area was equal to the area of compression, and that the load on the soundboard was 50 grams, our predicted voltage response would be 5.7 mV.

	Voltage Measured (mV):
Baseline Peaks	11 to -11
Agitated Peaks	13 to -13

**Fig. 15.** Measured voltage on an MSO688 Oscilloscope

As shown in figure 15, the large IDT gave a peak-to-peak voltage output which oscillated between 11 to -11 mV when attached to the spot shown on figure 5. We believe this response was affected by the wires used to connect the IDT to our oscilloscope, as well as ambient 60 Hz noise around us-- the measurements were taken in an electromagnetics lab. When the low E string of the guitar was played, the displaced soundboard agitated our IDT, producing a new response that oscillated between 13 and -13 mV. The total increase in voltage, peak-to-peak, was approximately 4mV, about 70% of our predicted value.

In a separate experiment, we moved the transducer to a different part of the soundboard, and noticed an abnormal interaction. When we manually agitated the guitar soundboard while keeping the IDT in place, the IDT did not output any notable responses-- except for when we agitated one small region, just above the mylar tape. Figures 16 and 17 depict the oscilloscope captures for the transducer, with figure 16 showing the baseline capture, and figure 17 showing the voltage capture when “touching” the abnormal spot. Figure 18 depicts the setup, and we’ve experimentally eliminated the possibility of movement in the wires, movement in the IDT, extraneous electrode finger responses, and confounding factors due to the mylar tape causing

these inconclusive results. Further work is required in determining the most electrically responsive regions on the guitar's soundboard, but we currently believe these inconclusive results are related to the unique geometry of the bracing underneath the soundboard.

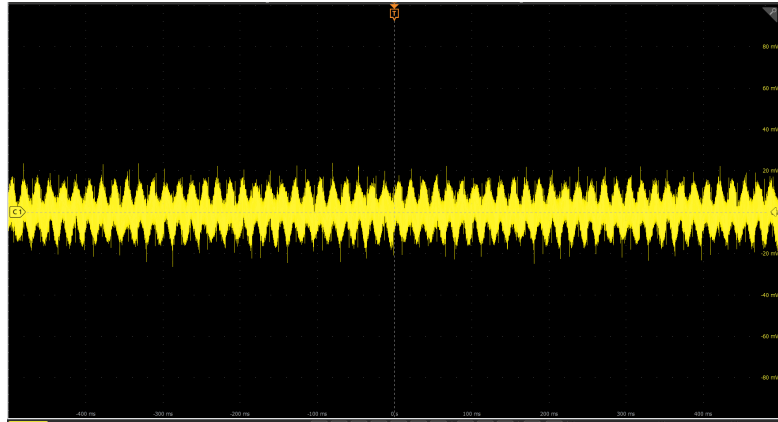


**Fig. 16.** 800ms oscilloscope capture of baseline transducer voltage in mV, limited to 20 MHz bandwidth

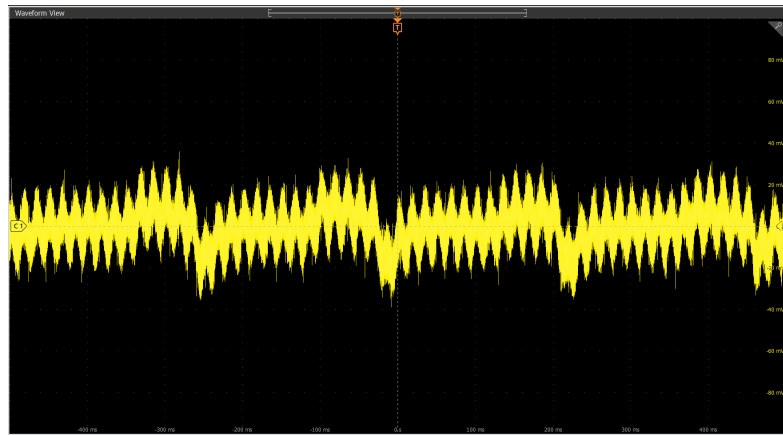


**Fig. 17.** 800ms oscilloscope capture of transducer voltage in mV while agitating the abnormal soundboard region, limited to 20 MHz bandwidth

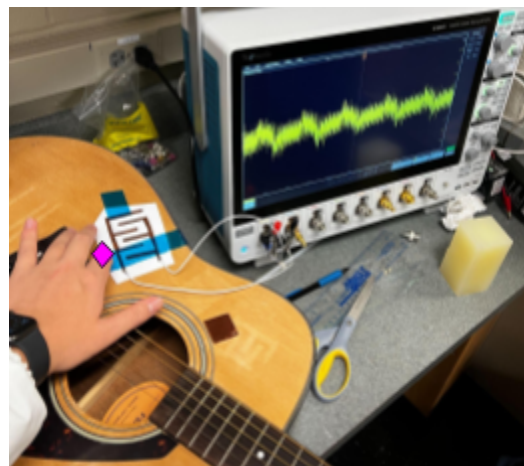


**Fig. 18.** Oscilloscope setup, annotated to depict the abnormal soundboard region with a pink diamond

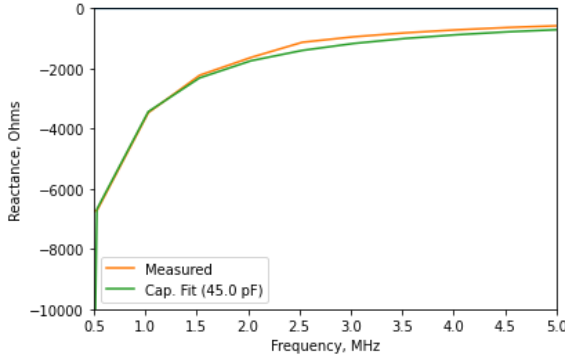


**Fig. 19.** Reactance of short transducer over a short cable

The orange line in figure 19 depicts a graph of magnitude vs. frequency. We obtained our data to plot the reflection coefficient from a N9918A FieldFox Microwave Frequency Analyzer, which was manually calibrated beforehand with a load and a short. This data was then converted to an impedance, which was graphed against capacitance, depicted by the green line. The “matching” value for the capacitance against the collected data was at 45 pF; however, the data we collected also includes the cable capacitance in the reflection coefficient measurement. This is because the network analyzer calibration had its “reference plane” set at the end of the test cable, which does not include the short cable attached to the transducer.

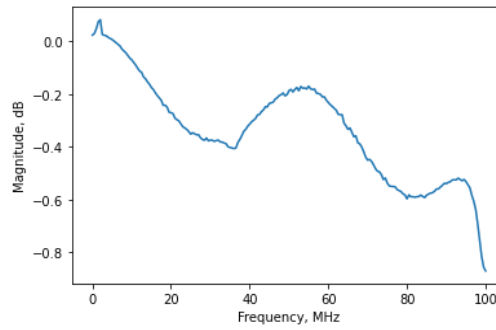


**Fig. 20.** Reflected power for short IDT on styrofoam

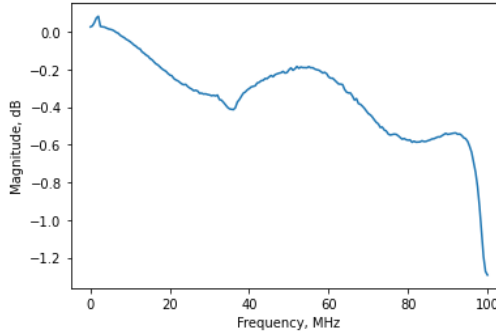


**Fig. 21.** Reflected power for short IDT on Rexolite

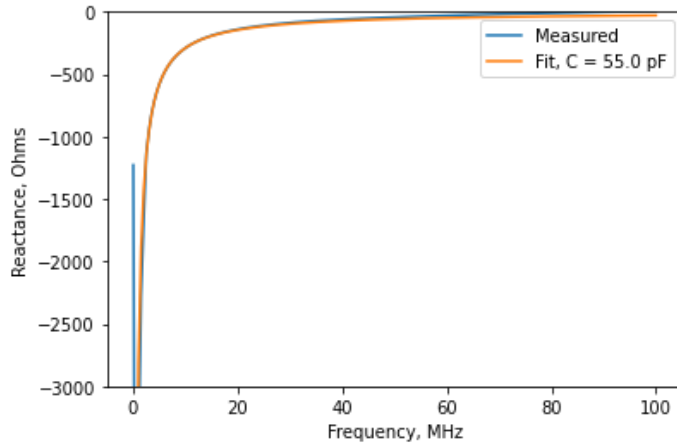


**Fig. 22.** Capacitive Reactance of IDT on Styrofoam

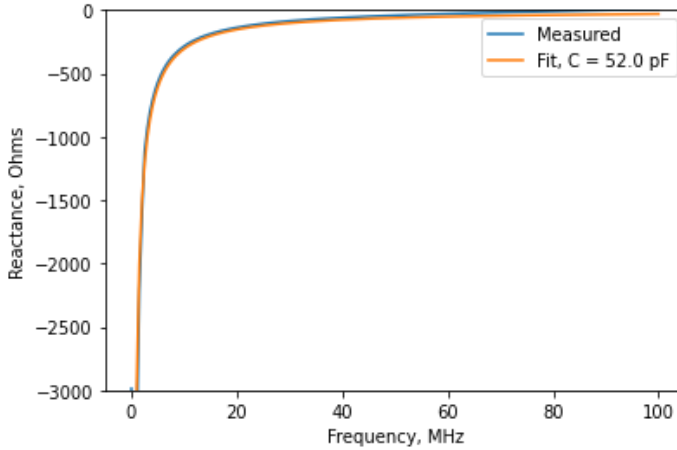


**Fig. 23.** Capacitive Reactance of IDT on Rexolite

Figures 20 and 21 depict a similarly-shaped reflected power curve of the large IDT when placed on styrofoam and Rexolite. However, the curve values differ in the 100 MHz range with styrofoam producing a response slightly larger than -0.8 dB and Rexolite producing a response slightly larger than -1.2 dB. The reduced reflection of rexolite may indicate an increased absorption, as shown by figure 21 when compared to styrofoam's reflection, as depicted by figure 20. The tests conducted between figure 20-23 are significant because they confirmed our beliefs that the coaxial cable's capacitance overpowered the capacitance we intended to measure in figure 13. Additionally, these tests verified our IDT's function as a capacitor (due to reactance being negative), further supporting our previous capacitance and voltage measurements.

## 2.4 Printing Conductive Electrodes

Our work has both quantified the electric properties of the guitar's soundboard, and investigated an effective transducer to pick up these vibrations. We now propose the plausibility of printing these electrodes through a modified inkjet with silver nanoparticle ink onto substrate which can then be attached to the guitar's soundboard. The main benefit of this electrode fabrication method is that it is scalable, cheap, and easily adaptable. The Media Lab explored the aesthetic capabilities of electrode printing for instruments in 2013, and GTRI conducted internal tests for conductive inkjet printing in 2013 as well [24].

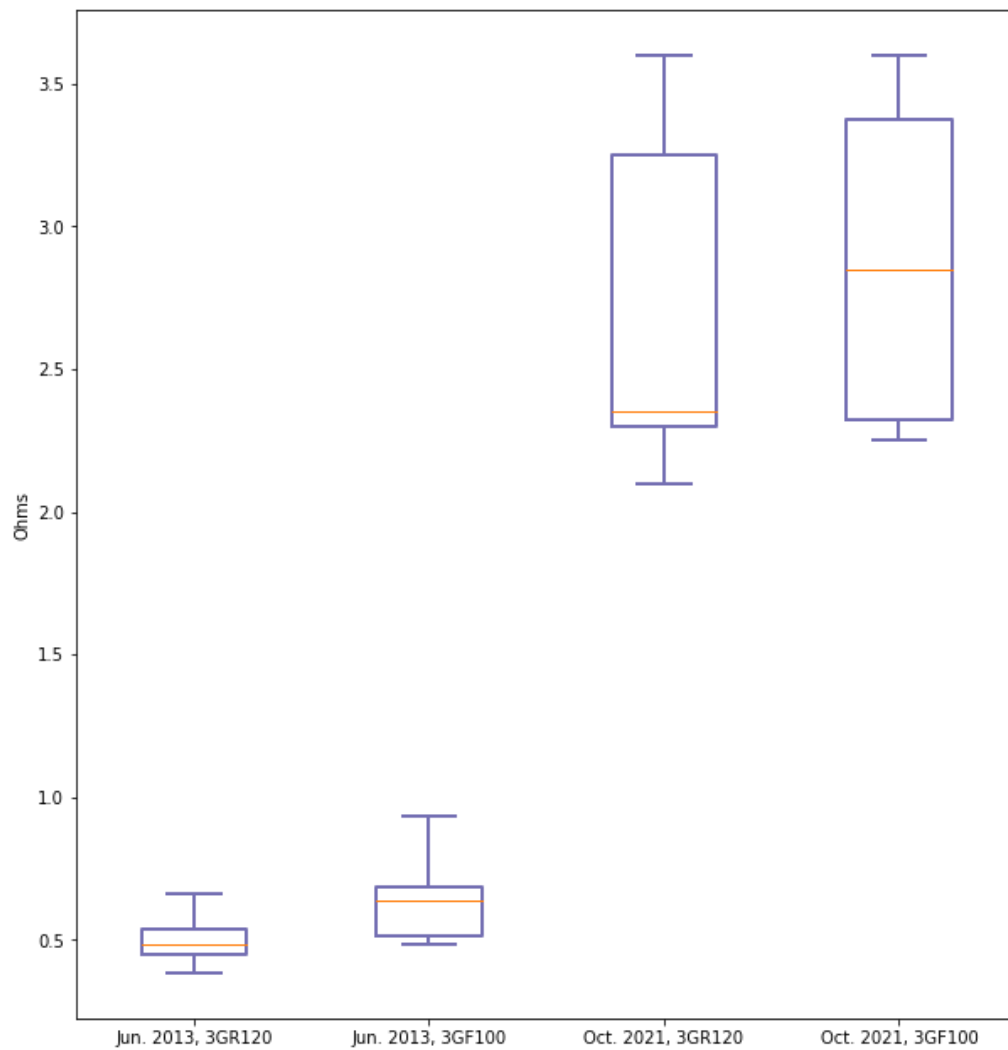


**Fig. 24.** Resistivity of 1" L x 1/2" W strips of silver nanoparticle ink, sorted by date and substrate

We measured the resistivity of 6 strips for each type of substrate, in Ohms, on a Fluke 115 multimeter. In the measurements conducted by GTRI in 2013, type 3GR120 substrate contained the least resistivity and variance. This trend remains consistent with the measurements conducted slightly over 8 years later. Over time, both substrates increased in average resistivity with the 3GR120 substrate increasing by approximately less than a factor of 5, and the 3GF100 substrate increasing by roughly the same factor. We estimate that printed electrodes for the guitar's soundboard will have a lifespan of approximately a year before any substantial impacts on performance are detected. Although this time period appears short, it's important to note the sustained benefits of these electrodes because they are able to be printed and utilized within minutes at a low cost, while also supporting an infinite combination of designs.

### 3. Conclusions

This project first proposes a new method for amplifying guitars by converting piezoelectric responses to sound, which can be extrapolated to all polymer-based instruments including the piano, violin, and synthetically-printed instruments too. Then, we examined previous vibrometry measurements to create equation 3, a model for strain energy, to determine that the largest displacement and maximum energy for the transducer on the soundboard exists on  $x = 0$  meters, or the center of the bridge of the guitar's soundboard. This point is depicted by the pink dot on figure 5. Both Fukada's and Bazhenov's experiments, conducted between the 1950s-60s, established the piezoelectric properties of wood; our initial experiments verified that this property remains consistent with standard, unaltered cuts of wood used in previous experiments despite our guitar's soundboard top being laminated. The wooden bracing underneath the soundboard was also shown to have minimal effects on the electric properties of the soundboard top. We successfully modeled capacitance and voltage through equations, and experimentally verified our predictions with an accuracy of  $\geq 95.4\%$  for all measurements pertaining to the parallel plate transducer. After conducting these measurements, we then designed an IDT and determined its electric properties by placing it on wood and Rexolite. The initial results were skewed due to our cable's capacitance dominating the IDT's capacitance, so we modified future experiments to use a minimally disruptive cable. We predicted and measured capacitance for our IDT, with a 0.23% margin of error. The peak-to-peak voltage response was

found to be approximately 4mV, about 70% of our predicted value of 5.7mV. During our experiments, we discovered an abnormal spot on the soundboard which gave a unique voltage response, depicted in figure 17. For measurements conducted on the oscilloscope, we believe Johnson noise partially distorted our results. The IDT's reactance and reflected power were measured and compared for both air and Rexolite, to prove its function as a capacitor. We also showed that the comparative capacitive impedance, shown by figure 22, produces a slightly larger difference than the actual dielectric constant between air and Rexolite. After demonstrating the validity and reliability of our IDT for picking up the guitar's displacements, we proposed a cheap, adaptable, and aesthetic solution for fabricating these electrodes: off-the-shelf inkjet printing. The longevity of this method for printing conductive electrodes was verified by comparing data collected on silver nanoparticle electrodes printed in 2013.

#### 4. Future Work

Our work both quantifies and proposes an accurate, replicable model for the future construction of IDTs. The methodologies used can be applied to future works on other classes of instruments as well; more specifically, wood-based instruments or other molecularly similar instruments. We are particularly interested in the synthetic manufacture of polymer-based instruments, which could lead to an even finer control on the electric responses one might wish to manipulate. We successfully predicted and quantified a voltage response to be picked up from the IDT attached to the instrument; however, this voltage was in millivolts. To create a pickup that successfully converts these responses to sound, we would need a microvolt amplifier that does not distort the input from the IDT-- otherwise, intended sound would be misrepresented. Microvolt amplifiers are relatively inexpensive, with some starting from \$6 [25]; future work demands a survey on amplifiers to determine microvolt amps that receive IDT inputs with and produce a clean output response. Another issue with these amplifiers lies in the fact that we have to filter stray electromagnetic signals to successfully convert our inputs to sound. An approach to both these problems is to disregard the amplifier's quality entirely, and turn to a software-based solution. We believe an AI-trained model could filter these EM signals and digitally "enhance" the resolution of the amplified, distorted input to produce a clear output.

## 5. References

- [1] R. C. D. Paiva, J. Pakarinen, and V. Välimäki, "Acoustics and Modeling of Pickups," *Journal of the Audio Engineering Society*, vol. 60, no. 10, pp. 768–782, Oct. 2012.
- [2] E. Fukada, "Piezoelectricity as a fundamental property of wood," *Wood Science and Technology*, vol. 2, no. 4, pp. 299–307, 1968, doi: 10.1007/BF00350276.
- [3] V. A. Bazhenov, *Piezoelectric properties of wood: Authorized translation from Russian*. New York: Consultants Bureau, 1961.
- [4] A. V. Mamishev, K. Sundara-Rajan, F. Yang, Y. Du, and M. Zahn, "Interdigital sensors and Transducers," *Proceedings of the IEEE*, vol. 92, no. 5, pp. 808–845, May 2004.
- [5] R. Hay, "FREQUENCY ADJUSTABLE SURFACE ACOUSTIC WAVE OSCILLATOR ,," 26-Apr-2011.
- [6] G. Caldersmith, "Guitar as a reflex enclosure," *Journal of the Acoustical Society of America*, vol. 63, no. 5, pp. 1566–1575, 1978
- [7] B. E. Richardson and G. P. Walker, "Mode coupling in the guitar," in Proceedings of 12th International Congress of Acoustics, vol. 3, K3-2, Toronto, Canada, 1986.
- [8] M. K. Lee, M. H. Fouladi, and S. N. Namasivayam, "Mathematical modelling and acoustical analysis of classical guitars and their soundboards," *Advances in Acoustics and Vibration*, pp. 1–11, Dec. 2016.
- [9] "Audio spectrum," *Teach Me Audio*, 25-Apr-2020. [Online]. Available: <https://www.teachmeaudio.com/mixing/techniques/audio-spectrum>. [Accessed: 07-Oct-2021].
- [10] M. J. S. Lowe and D. S. Ballantine, "Lamb Waves - an overview ,," *ScienceDirect*, 2001. [Online]. Available: <https://www.sciencedirect.com/topics/physics-and-astronomy/lamb-waves>. [Accessed: 20-Oct-2021].
- [11] Inta R. The Acoustics of The Steel String Guitar. PhD Thesis, School of Physics, The University of New South Wales, Sydney, Australia; 2007. p. 152–290
- [12] E. Fukada, "Piezoelectricity of Wood," *Journal of the Physical Society of Japan*, vol. 10, no. 2, pp. 149–154, Feb.1955, doi: 10.1143/JPSJ.10.149.
- [13] W. W. Barkas, R. F. Hearmon, and G. H. Pratt, "Electrical resistance of Wood," *Nature*, vol. 151, no. 3820, pp. 83–83, Jan. 1943.
- [14] T. Nakai, N. Igushi, and K. Ando, "Piezoelectric behavior of wood under combined compression and vibration stresses I: Relation between piezoelectric voltage and microscopic deformation of a sitka spruce (*picea sitchensis carr.*)," *Journal of Wood Science*, vol. 44, no. 1, pp. 28–34, Jul. 1998.
- [15] S. L. Zelinka, S. V. Glass, and D. S. Stone, "A Percolation Model for Electrical Conduction in Wood With Implications for Wood-Water Relations," *Wood and Fiber Science*, vol. 40, pp. 544–552, May 2008.
- [16] A. Silker and Y. Yu, "Elastic Constants for Hardwoods Measured from Plate and Tension Tests," *Wood and Fiber Science*, vol. 25, no. 1, pp. 8–22, Jan. 1993.
- [17] B. Richardson, *Modes of Vibration on Guitar Soundboard*. Lord Grey, 2003.
- [18] B. Richardson "Guitar Making- The Acoustician's Tale," Proceedings of the Second Vienna Talk, Sept. 19-21, 2010, University of Music and Performing Arts Vienna, Austria. 2010.
- [19] W. James, "Dielectric properties of wood and hardboard: Variation with temperature, frequency, moisture content and grain direction.,," Forest Products Laboratory, U.S. Department of Agriculture, 2005.
- [20] D. Trent, "The Ultimate Yamaha F335 acoustic guitar review," *Guitar Space*, 02-Sep-2021. [Online]. Available: <https://guitarspace.org/acoustic-guitars/the-ultimate-yamaha-f335-acoustic-guitar-review/>. [Accessed: 17-Oct-2021].
- [21] N. S. Mazlan, M. M. Ramli, M. M. Abdullah, D. S. Halin, S. S. Isa, L. F. Talip, N. S. Danial, and S. A. Murad, "Interdigitated electrodes as impedance and capacitance biosensors: A Review," in *AIP Conference Proceedings*, vol. 1885, no. 1, Sep. 2017.
- [22] A. Janeliauskas, "Design and modeling of surface acoustic wave sensor with staggered ID – tag ,," *Ultragarsas (Ultrasound)*, vol. 65, no. 2, pp. 24–29, 2010.
- [23] K.-ya Hashimoto, *Surface Acoustic Wave Devices in Telecommunications*. Berlin, Springer-Verlag, Berlin, Heidelberg, 2000.

- [24] N.-W. Gong, A. Zoran, and J. A. Paradiso, “Inkjet-printed conductive patterns for physical manipulation of audio signals,” *Proceedings of the adjunct publication of the 26th annual ACM symposium on User interface software and technology*, Oct. 2013.
- [25] “AD620 Microvolt Millivolt Signal Amplifier Module 1.5-1000 Gain Adjustable,” *Amazon*, 14-Jun-2017. [Online]. Available: <https://www.amazon.com/Icstation-AD620-Microvolt-Amplifier-Adjustable/dp/B072N57L7H>. [Accessed: 07-Nov-2021].